IOP PUBLISHING PHYSICS IN MEDICINE AND BIOLOGY

Phys. Med. Biol. **54** (2009) R99–R115 doi:10.1088/0031-9155/54/21/R01

TOPICAL REVIEW

Interaction of MRI field gradients with the human body

P M Glover

The Sir Peter Mansfield Magnetic Resonance Centre, School of Physics and Astronomy, University of Nottingham, Nottingham NG7 2RD, UK

E-mail: paul.glover@Nottingham.ac.uk

Received 8 July 2009, in final form 14 September 2009
Published 14 October 2009
Online at stacks.iop.org/PMB/54/R99

Abstract

In this review, the effects of low-frequency electromagnetic fields encountered specifically during magnetic resonance imaging (MRI) are examined. The primary biological effect at frequencies of between 100 and 5000 Hz (typical of MRI magnetic field gradient switching) is peripheral nerve stimulation, the result of which can be a mild tingling and muscle twitching to a sensation of pain. The models for nerve stimulation and how they are related to the rate of change of magnetic field are examined. The experimental measurements, and analytic and computational modelling work in this area are reviewed. The review concludes with a discussion of current regulation in this area and current practice as both are applied to MRI.

(Some figures in this article are in colour only in the electronic version)

Introduction

The safety aspects of magnetic resonance imaging (MRI) scanners have been uppermost in the minds of their developers from the earliest pioneering experiments. The BBC popular science programme 'Tomorrow's World' cameras were present when Sir Peter Mansfield climbed in to his first whole-body imaging magnet. Sir Peter announced to camera that any cardiac arrest, should it happen, would be immediate when the scan started. However, he had made some calculations and he thought it unlikely. Of course, as we now know, there were no acute effects and the programme was broadcast and paper published in 1978 (Mansfield *et al* 1978). This anecdote serves to underline some of the important points and questions which are discussed in this review, namely induced currents flowing around the body and, above some threshold, biological effects that can range from tingling sensations to cardiac arrest (Reilly 1989, Schenck *et al* 1983). However, there are a number of factors which prevent the accurate prediction of the magnitude of switched magnetic field gradients required to induce nerve stimulation for a specific individual within a particular scanner (Den Boer

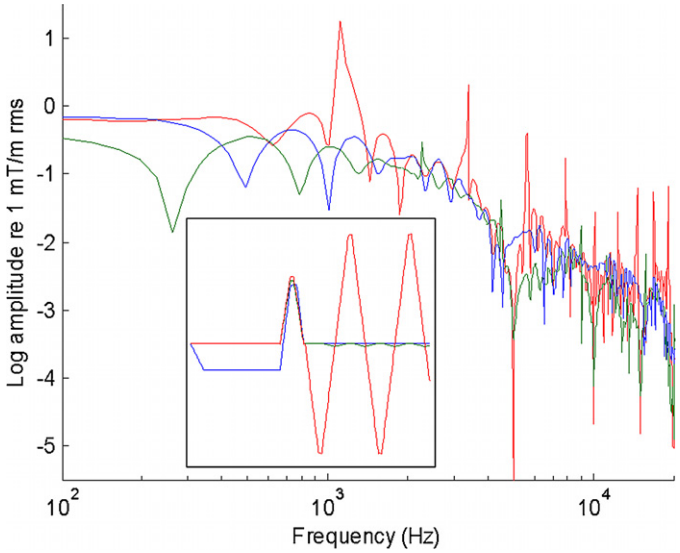

Figure 1. Spectral content of the magnetic gradient field for a typical echo planar imaging sequence. Inset is part of the gradient sequence showing the slice selection, readout (switched) and phase encoding gradients.

et al 2002). Additionally, there are difficulties in understanding the exact mechanisms which link induced electric fields to nerve axon or muscle tissue depolarization—these could be absolute in magnitude or spatial derivatives of the electric field (Maccabee *et al* 1993). The biological processes are time and frequency dependent and are generally nonlinear in their response (i.e. a threshold has to ssssssbe reached) to applied fields (Lapicque 1909). Together with subject-dependent perceived response it is therefore not always possible to predict the thresholds for a specific subject with any great accuracy.

Magnetic field gradients are an essential part of the process of standard clinical MRI. These are produced by switchable electromagnetic coils which provide a linear varying spatial dependence of magnetic field along a particular axis. These are switched in particular sequences to encode the spatial position of the signal to give an image. The ability to switch these gradients quickly gives several performance advantages to the MRI process. High levels of gradient are also desirable. A typical modern clinical scanner is able to generate 40 mT m^{-1} at a switching rate of up to 200 T m^{-1} s^{-1}. Hence, the gradient can be switched from zero to maximum in $\sim$200 μs. Even higher values of gradient magnitude are usually desirable for diffusion-weighted imaging. Gradient waveforms employed in an imaging sequence are usually trapezoidal in nature and have variable overall pulse lengths and orientations (see the inset of figure 1). This complicates the relationship between sequence used and the likelihood of nerve stimulation. Gradients may be applied along different axes either together or separately. These considerations make comparison (and hence interpretation) of MRI nerve stimulation with *in vitro* experiments difficult.

Because of the difficulties in calculating or measuring exact electric fields, the way of dealing with the problem of peripheral nerve stimulation (PNS) has been to take data based on experimental evidence and produce a figure of rate of change of magnetic field (dB/dt) beyond which the scanner cannot go (during a standard sequence) (Bourland *et al* 1999, Budinger *et al* 1991, Ham *et al* 1997). The values used may scale with gradient axis but will not usually take

account of body position and geometry. It may be possible, under certain circumstances, for identical sequences on two different scanners to have different PNS responses because of the slight spatial differences in applied magnetic gradient fields. As such the 'assumed' threshold of PNS (based on a particular value of dB/dt) may be either far too conservative and therefore compromises scanner efficacy or too lenient and give an unacceptable rate of PNS effects.

In this review, the current understanding of the effects of magnetic field gradient switching on the human body will be discussed. This will start with some basic theory for both electromagnetism and interactions with biological systems. The spatial nature of the gradients will be discussed together with a review of numerical methods of calculating induced currents due to switched gradients. The review concludes with a discussion of current regulations as they are applied to MRI.

Electromagnetic theory

It is useful to include a short resume of the electromagnetic theory of induction of electric fields. Faraday's law of electromagnetic induction states that the electro-motive force (EMF) generated in a circuit is given by the negative rate of change of the total flux, Φ, linked by the circuit,

$$\mathrm{EMF} = -\frac{\mathrm{d}\Phi}{\mathrm{d}t} = -\frac{\mathrm{d}}{\mathrm{d}t}\int \mathbf{B}\cdot\mathrm{d}\mathbf{S},$$

where $\mathbf{B}$ is the magnetic flux density in tesla and $\mathbf{S}$ is the vector defining the surface defined by the closed circuit. The total EMF is equivalent to the total integrated electric field $\mathbf{E}$ around the circuit and is related to the magnetic field by use of Stokes' theorem,

$$\int \mathbf{E}\cdot\mathrm{d}\mathbf{l} = \int (\nabla\times\mathbf{E})\cdot\mathrm{d}\mathbf{S} = -\frac{\partial}{\partial t}\int \mathbf{B}\cdot\mathrm{d}\mathbf{S},$$

and hence

$$\nabla\times\mathbf{E} = -\frac{\partial\mathbf{B}}{\partial t}.$$

Gradient switching occurs over a frequency range of a few hundred hertz to several kHz. The spectral content of an echo planar imaging (EPI) sequence is shown in figure 1.

At low frequency and as the conductivity, σ, of biological tissue is of the order of 1 S m^{-1}, the system can be regarded as purely quasi-static, i.e. wave effects can be disregarded. In addition, the magnitude of any induced current (including displacement current) will not be high enough to influence or modify any applied magnetic field (i.e. no eddy current-like effects). In a complex heterogeneous object, such as a human body, the induced electric field is subject to constraints imposed by the boundary conditions between volumes of different conductivity and permittivity. At any boundary, the tangential components of the electric fields ($\mathbf{E}_1$ and $\mathbf{E}_2$) on either side must be equal. From the continuity equation then the current flowing through the surface on either side must also be equal; hence, $\sigma_2\mathbf{E}_2\cdot\hat{\mathbf{n}} - \sigma_1\mathbf{E}_1\cdot\hat{\mathbf{n}} = 0$, where $\hat{\mathbf{n}}$ is the unit vector normal to the surface and σ_1 and σ_2 are the conductivities on either side of the boundary. In order that this condition is met then a surface charge is developed equal to $\varepsilon_2\mathbf{E}_2\cdot\hat{\mathbf{n}} - \varepsilon_1\mathbf{E}_1\cdot\hat{\mathbf{n}}$, where ε_1 and ε_2 are the tissue permittivity on either side of the boundary. At a frequency ω, where $\sigma/\omega\varepsilon \gg 1$ (defining a conductor and quasi-static conditions), although the surface charge is affected by tissue permittivity, the net current flow is not. However, for a semi-permeable cell membrane, the ratio of ε/σ (given by the product of the resistance and capacitance per unit area) is defined as the membrane time constant τ_m and is of the order of 1000 μs (Cartee and Plonsey 1992). Thus, it is likely that the threshold

for cell depolarization with induced fields will have a strong frequency dependence within the band of frequencies covered by gradient switching.

It is possible to define magnetic and electric fields in terms of a vector potential, $\mathbf{A}$, and a scalar potential, V. These potentials can be useful in solving particular problems in electromagnetism (Jackson 1998). The electric field can be written as $\mathbf{E} = -\nabla V - \mathrm{d}\mathbf{A}/\mathrm{d}t$, where the vector potential is defined such that $\mathbf{B} = \nabla \times \mathbf{A}$. For a uniform time varying magnetic field applied across a uniform conductive sphere, the vector potential may be used such that $\mathrm{d}\mathbf{A}/\mathrm{d}t = \frac{1}{2}\mathbf{r} \times \mathrm{d}\mathbf{B}/\mathrm{d}t$. In the case of a magnetic field B_z along the z-axis, the electric field at a distance r from the z-axis within the sphere is given by $E_\phi = \frac{1}{2}r\mathrm{d}B_z/\mathrm{d}t$. The current density, $\mathbf{J}$, can then be found from $\mathbf{J} = \sigma\mathbf{E}$. In this spherical example, the current is always exactly tangential anywhere on the surface so the boundary conditions are always maintained without an additional surface charge. This simple calculation has been used as the basis for approximation of the magnitude of current flowing in the human body (Irnich and Schmitt 1995). However, the inhomogeneity of conductive volumes and variable current paths in the human body can modulate this approximation quite significantly. An obvious example would be making a small break in a ring of conductor which has an induced EMF. A change in conductivity at a single point on the ring influences the electric field on the other side of the ring. A further complication is the non-uniformity of the magnetic field thus breaking the condition imposed on the calculation of the vector potential above. It is usual to assume that the subject remains stationary for calculation of induced fields due to gradient switching. Any movement of the body in the magnet (for example due to blood flow or limb movement) can usually be disregarded. The product $\mathbf{v} \times \mathbf{B}$, where $\mathbf{v}$ is the velocity, will produce an additional electric field component, which may be added, but the frequency components due to movement usually lie in the range 0–30 Hz. The induced electric fields at these ultra-low frequencies are responsible for magneto-phosphenes, vertigo and metallic taste sensations, and are not discussed in detail in this review.

Magnetic resonance imaging gradients

For MRI, the gradients are defined purely as linear variations in B_z along each of three axes: $G_x = \frac{\mathrm{d}B_z}{\mathrm{d}x}$; $G_y = \frac{\mathrm{d}B_z}{\mathrm{d}y}$ and $G_z = \frac{\mathrm{d}B_z}{\mathrm{d}z}$. Clearly, to satisfy $\nabla \cdot \mathbf{B} = 0$ and $\nabla \times \mathbf{B} = 0$ within the volume of the coil, there are additional spatial terms in B_x and B_y. Whilst the latter have very little effect on the imaging, their presence will contribute to the current flowing in the body of the subject and have to be included. Figure 2 shows the axial variation in the magnetic field from a typical whole body scanner. Outside the region of linear gradient, the maximum value is soon reached and thereafter the level falls rapidly to zero. The linear region is defined by the diameter of the spherical volume (DSV) of homogeneous gradient. The imaging volume is usually centred on the zero-crossing of the gradient profile—at the iso-centre of the magnet. A subject would be positioned so that the anatomy of interest would be at that position. It is easy to see that for a head scan, there will be a maximum magnetic field in the thorax and vice versa. For switching of G_z, the induced electric field would preferentially form an azimuthal pattern scaling with radius. For switching of G_x or G_y (transverse gradients), the induced electric field is more complex with a transverse current flowing even at the iso-centre ($x = y = z = 0$) (Glover and Bowtell 2007). Measurements, theoretical analysis and numerical simulation demonstrate the behaviour of the induced electric fields due to gradient switching.

It is essential to switch the gradients on and off quickly to encode the image or other effects such as diffusion weighting. The gradient field can switch the polarity of a gradient at

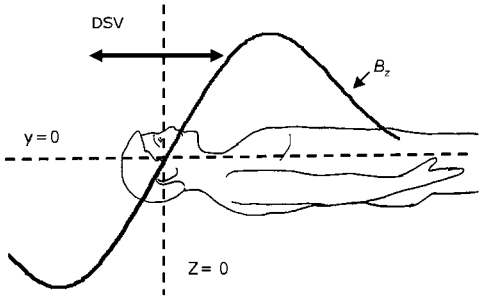

Figure 2. Typical form and extent of the magnetic field for an axial gradient. The central linear region is used for imaging which may cover a 40 cm diametrically spherical volume (DSV).

maximum magnitude in around 200–300 μs. The typical inductance of a whole-body gradient set may be of the order of 200 μH. Modern switch-mode power supplies are able to provide several hundred amps at up to 750 V. Faraday shielding is provided between the subject and the gradient coil to ensure that no capacitively coupled currents can flow through the body. The gradient slew rate on a whole-body system will be limited to typically 200 T m^{-1} s^{-1}. The ability for power amplifiers to drive large currents into inductive loads diminishes with increasing frequency. A whole-body scanner is therefore capable of inducing PNS in a subject unless the slew rates are restricted to below the threshold value. The default setting on clinical systems is to set a conservative limit for avoiding PNS. The MRI sequence usually comprises a set of gradient reversals and flat topped pulses as shown in figures 1 and 3. It is important to remember that the induced electric field is proportional to the derivative of the gradient shape. For example, an MR physicist might refer to a 1 ms pulse but the nerve cell would 'experience' two pulses of 150 μs duration spaced 1 ms apart and opposing polarity as shown in figure 3. The pulse sequences used vary widely in their nature in terms of type, length and duration. For the very fastest of EPI sequences, which are most likely to induce PNS, the gradients will be switched and/or reversed to their maximum levels up to 64 times in 30 ms. Most of the experimental work reported in the literature uses a repetitive pulse sequence of this nature (Cohen *et al* 1990, Zhang *et al* 2003). Sinusoidal magnetic fields are rarely used in MRI but have the advantage of being at a single frequency so easier for threshold experiments and interpretation. It appears that simple scaling of thresholds related to actual pulse shape and frequency can be used (Irnich and Schmitt 1995, Mansfield and Harvey 1993). The maximum frequency which has to be considered is around 10–20 kHz which is well below the frequencies where significant tissue heating will occur due to induced currents, i.e. at radio-frequencies (Collins *et al* 1998).

Electric field interactions with the nervous system

Electrically excitable tissue (such as cardiac muscle or nerve axons) can be modelled by assuming a one-dimensional cable equation (Rattay and Aberham 1993, Ruohonen *et al* 1996a, 1996b). The spatial and temporal behaviour of the trans-membrane potential V_m is given by

$$V_m + \tau_m \frac{\partial V_m}{\partial t} - \lambda^2 \frac{\partial^2 V_m}{\partial z^2} = -\lambda^2 \frac{\partial E_z}{\partial z},$$

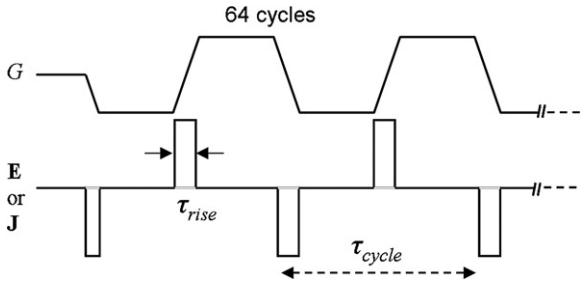

Figure 3. A typical switched gradient waveform showing the relationship to induced fields.

where τ_m is the membrane time constant, λ is a length constant and E_z is the driving term electric field along the length of the fibre. This electric field can exist due to either potentials applied to nearby electrodes or an electric field induced by a time varying magnetic field. The equation can be solved for simple linear fibres and shown to be in excellent agreement with data from *in vitro* experimental work (Basser and Roth 2000, Ueno *et al* 1984). The spatial and temporal dependence of nerve fibre de-polarization of the excitable tissue can be predicted (Maccabee *et al* 1993). Electrodes placed near the nerve produce a large spatial variation in the electric field which produces a large 'driving term' in the cable equation above. For example, the cathodal stimulation can be shown to be approximately five times more effective than anodal stimulation if the electrode is placed more than a few length constants from the fibres (Basser and Roth 2000). Cartee and Plonsey (1992) show from an analytic approach based on the cable equation and intracellular potentials that not only is the spatial applied electric field relevant but also the trans-membrane potential time constant is related to the geometry of both the nerve cell and the location of the stimulus. The length constant λ is related to the fibre diameter and the intracellular, extracellular and membrane resistances. The resulting effective time constant of the cell can be much smaller than τ_m for an extracellular electrode stimulus. The further away the electrode the longer the time constant.

Experiments have been carried out on single nerve fibres *in vitro* using small localized magnetic stimulators (Di Barba *et al* 2007, Ruohonen *et al* 1996a, Ueno *et al* 1984). This type of stimulator produces a large spatial derivative of electric field along the direction of the fibre. These experiments are fully consistent with the electric potential experiments when the spatial nature of the electric field is considered. In some experiments, the electric field is modified by adding non-conductive blocks which serve to increase the spatial rate of change of induced electric field (Maccabee *et al* 1993). Experiments of this nature indicate that nerve depolarization is mediated solely through the spatial components of the induced electric field and is not a function of magnetic field magnitude in itself or a direct magnetic effect. The *in vitro* situation is unlike that in the human body where the gradient magnetic fields are comparatively more uniform and hence the spatial derivative of the electric field will be much smaller. However, if the fibre is bent in a uniform electric field then the fibre can be excited by the effective spatial derivative of the electric field. Localized behaviour of electric fields due to non-homogeneous conductivity can give rise to higher effective electric fields. This may be particularly true where fibre tracts pass by or through volumes of lower conductivity, in tissue or at skin surfaces. Although the cable equation may predict the behaviour of a single fibre in isolation, there are many possible orientations and current paths in the human body.

Many researchers have attempted to model the electrical activity and response to electrical fields of the heart. Cardiac cells act as a 3D cable and can be written as such. However,

to simplify matters, the tissue can be modelled as a bio-domain, i.e. having no fine cellular structure (Basser and Roth 2000). Using this method, the models can predict the experimentally observed cathode and anode electrode behaviour. Despite a good understanding of the electrical response of the nerve and other excitable tissue, we have the situation where, due to non-localized current flow, there is some difficulty in translating these *in vitro* observations to the whole human organism.

In order to simplify the situation for *in vivo* experiments, it is easier to introduce a strength–duration relationship based on either the electric field or the applied magnetic field. This was first attempted by Weiss (1901) who noted that there was a relationship between the charge flow (time integral) and the stimulus duration. This may be written as $\int^{\tau_s} E\mathrm{d}t = E_r(\tau_s + \tau_c)$, where E_r is the rheobase (the minimum electric field to produce stimulation), τ_c is the chronaxie (the stimulation duration τ_s which is required to double the stimulation threshold) as defined by Lapicque (1909). Written in terms of the electric field, the stimulation threshold for a rectangular pulse based on this strength–duration relationship is given by $E_s = E_r\left(1 + \frac{\tau_c}{\tau_s}\right)$. Bailey and Nyenhuis (2005) derive a similar relationship using magnetic field terms instead of electric field. It is useful to note that this hyperbolic relationship fits the experimental data more closely than an exponential-based relationship as would be expected by an exponential time constant (Irnich and Schmitt 1995, Schaefer *et al* 2000). The chronaxie parameter is known to vary with electrode size in electrophysiology which is consistent with the work of Cartee and Plonsey (1992) discussed previously. It is therefore unreasonable to expect that chronaxie will have a unique value for all types and geometry of stimulation *in vivo*. However, knowing the chronaxie and rheobase levels for a particular geometry and subject gives an accurate prediction of stimulation over a range of applied pulse lengths, frequencies and levels (Den Boer *et al* 2002, Schaefer *et al* 2000).

More usually in the MRI safety literature the time-dependent stimulation threshold is written as a slew-rate-related (either $\mathrm{d}B/\mathrm{d}t$ or $\mathrm{d}G/\mathrm{d}t$) threshold, $\mathrm{SR}(\tau_s) = \mathrm{SR}_r\left(1 + \frac{\tau_c}{\tau_s}\right)$, where SR_r is the minimum slew rate (of the magnetic field or gradient) to stimulate the tissue. The variation of the rate of change of magnetic field with applied pulse length required for stimulation (determined from results in the literature cited here) is shown in figure 4. Figure 5 shows the range of effective minimum threshold for given chronaxie values. Whilst it is the electric field in the tissue which ultimately causes stimulation, a calculation based on the rate of change of magnetic field is more convenient for the setting of scanner parameters—assuming a fixed subject size. Clearly the scanned subjects do vary in size and position; thus there is a wide variation in the reported values of the rheobase and chronaxie in the reported literature for magnetic field-induced stimulation. Mansfield and Harvey (1993) and Irnich and Schmitt (1995) wrote the stimulation strength relationship in terms of a change in field as a linear function of pulse length. Zhang *et al* (2003) also used the linear form for the relationship between pulse length and threshold by re-writing the slew-rate relationship in terms of a gradient difference required for stimulation, $\Delta G_{\mathrm{stim}} = \mathrm{SR}_{\mathrm{min}}\tau_s + \Delta G_{\mathrm{min}} = \frac{E_r}{\beta}(\tau_s + \tau_c)$, where β is defined as the electric field per unit gradient slew rate at the point of stimulation. In this way, the chronaxie parameter may be evaluated from $\tau_c = \Delta G_{\mathrm{min}}/\mathrm{SR}_{\mathrm{min}}$ obtained from a fit to experimental data. The advantage in presenting the experimental data in this way is that the scanner hardware capabilities (operating area) can be superposed on a graph of gradient excursion shown in figure 6. The shaded area enclosed by the curves defines the operating area for which there is stimulation. Limitations with determining the magnetic field or gradient-related stimulation levels include their variation with the type of scanner and gradient coil used and subject-to-subject variability. This is readily demonstrated in the literature by examining the wide variation in rheobase and chronaxie values quoted as depicted in figure 5. Zhang *et al* (2003) show that subject variation moves the threshold curve (on the ΔG against τ_{c}

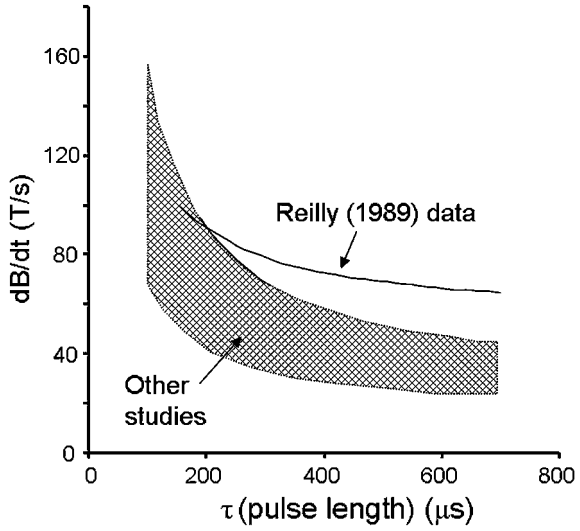

Figure 4. Graph showing typical minimum magnitude of dB/dt required for PNS against stimulus length. The hatched area indicates the ranges of experimental measurement from the cited literature. The Reilly (1989) data are generally higher than more recent studies. The variation in threshold is highly dependent on the geometry of subject, magnetic field generation as well as the subjective nature of the experiments.

graph) up and down demonstrating the relationship between these values and subject. A number of authors have published studies which attempt to find relationships between PNS threshold and geometry of the gradient and subject position. Faber *et al* (2003) attempted to provide experimental subject data dependent on position whilst switching gradients on one, two or all three axes simultaneously. Very usefully they attempt to correlate the major current paths around the trunk due to the various effective gradient orientations. They note that the gender of the subject affects the magnitude of the threshold but not the position of the stimulation. They ascribe the difference to the larger stature of males which increases the size of the current loops, and hence the magnitude of the current density will increase for the same applied gradient. Gradient coil designs can be specifically tailored to minimize the likelihood of thresholds being exceeded. Bowtell *et al* (2003) showed how the addition of a concomitant field coil (i.e. one which generates a magnetic field but does not generate a gradient term) can influence the stimulation threshold under certain conditions. The additional fields can be shown to alter the current paths around the body. Unfortunately, there may only be limited scope for such methods with only a small reduction possible. Mansfield and Haywood (2008) proposed that electric fields may be controlled by applying an external electric field. In this work, the external field is minimized by short-circuiting two plates. Clearly, there is scope for modifying the internal electric field in a subject by active application of an external field. However, it must be remembered that the induced electric field is not conservative whereas the external applied field is always conservative. The resulting cancellation cannot therefore be perfect in all cases and could even make the situation worse—in common with any active cancellation technique.

Magneto-phosphenes are perceived as light flashes and are thought to be retinal in origin as the induced electric field modulates the ionic currents flowing within the retina (Lovsund *et al* 1980a, 1980b). Magneto-phosphenes are perceived when electric fields and associated

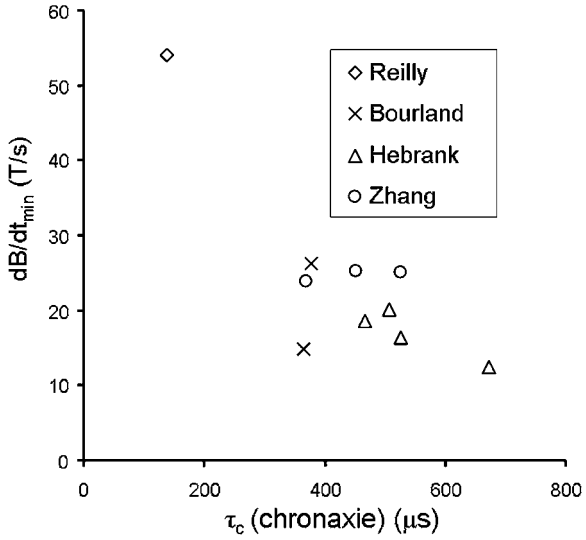

Figure 5. Graph showing the range of values for chronaxie and magnetic field rheobase given by the authors cited. This graph reflects the ranges shown in figure 4.

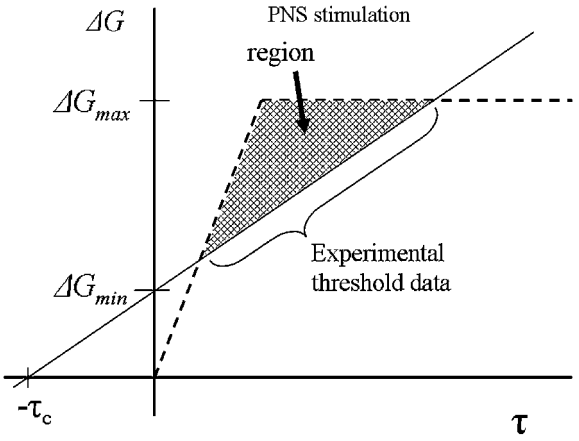

Figure 6. Graph showing rise in the magnetic field gradient required for a given rise time. The subject PNS threshold is characterized by the straight line defined by $-\tau_c$ and $\Delta G_{\min}$. The scanner operating area is defined by the dotted line. The hatched area indicates the region in which PNS will occur. Adapted from data given in Zhang *et al* (2003).

currents are well below those required for nerve cell depolarization (as discussed below). However, the frequency range over which magneto-phosphenes can be perceived is very narrow and centred on around 20 Hz. The change in magnetic field required for an optimal pulse rise time of 50 ms is around 100 mT. If this value were to be plotted onto a graph such as figure 6, then this would indicate that induction of magneto-phosphenes from gradient switching is not very likely for whole-body scanners. The magnetic field change required is too great to be achievable under normal conditions. The frequency components of the changing magnetic field are very small in the ultra-low-frequency range. In addition, vertigo

and metallic taste sensations are not perceived via the gradient switching process and the same argument can be applied (Cavin *et al* 2007, Glover *et al* 2007). For gradient switching and over time scales of greater than a few milliseconds, the electric field integrates to zero and thus the sensory mechanisms are unable to follow the changes.

Analytic and numerical modelling methods

The vector potential, **A**, can be directly calculated from the gradient coil current distribution for use in calculating the electric fields and current density (Bencsik *et al* 2003, Bowtell and Bowley 2000). It is usually an easier process to calculate (either numerically or analytically) a single scalar value of potential, V, at a point rather than the vector quantity **E**. It is important to stress that the quantities **A** and V are not absolutes in themselves; they are useful mathematical concepts. Only their spatial derivatives have a valid physical meaning and not their absolute magnitudes. As the current density generated in tissue with conductivity of the order of 1 S m^{-1} is not high enough to generate a magnetic field anywhere near the magnitude of the applied field, then it can be assumed that the magnetic field (and hence the vector potential) is equivalent whether or not the sample is present. Unlike the full-wave numerical models required for RF, the problem is somewhat simplified. A single frequency solution may be computed with simple linear extrapolation to all applicable frequencies (or rates of change in the time domain). For simple geometry such as flat plates, loops or spheres, an analytic solution may be formed (Bencsik *et al* 2002). It is usually assumed that (minus) the temporal derivative of **A** forms the basic electric field irrelevant of the value of conductivity. At every boundary point between domains, the condition on the current density, tangential electric fields and charge at the surfaces can be met by defining a continuous scalar potential throughout the domains. Because the problem is constrained and defined by its boundary conditions, boundary element methods (BEM) may be employed (Cobos-Sanchez 2007). The potential within each domain is then defined by the Poisson relation $\nabla^2 V = \rho/\varepsilon_0$ where ρ is a space charge (zero in the case of gradient switching). The BEM has its advantages when solving problems with few large-scale domains. Usually, because of the hetrogeneity of human tissue conductivity, it is easier to employ a finite element method. The same boundary equations are required but the potential is assumed to be constant across the volume of the element. The numerical methods taking the finite element approach are variously termed impedance methods (Deford and Gandhi 1985, Hart and Wood 1991, Nadeem *et al* 2003), scalar potential finite difference (Dawson *et al* 1997, So *et al* 2004) or quasi-static finite difference (Liu *et al* 2002). The impedance methods model the conductive sample as a set of interconnected nodes (one for each element) with resistors placed in between adjacent nodes. There are no interconnections between non-adjacent nodes which make the resulting set of equations simpler than a general network as would be found in a circuit simulator. Induced electric fields are added as additional voltage sources in series with the interconnecting nodal impedances. Thus, the boundary conditions are automatically preserved and current is conserved within the element volume. The system of equations can be written in terms of a linear matrix equation and solved with a number of techniques such as LU decomposition (Mishra *et al* 2006), successive over relaxation (SOR) (Liu and Crozier 2004), conjugate gradient (Dawson *et al* 1997) or bi-conjugate gradient (BiCGstab) (Wang *et al* 2008). Parallel methods may be applicable to some of the methods (Bomhof and van der Vorst 2000), and computation time for a single (human scale) calculation for current density due to gradient switching takes between a few minutes to an hour on a powerful computer platform depending on voxel resolution. In contrast, it is also valid to use finite difference time domain (FDTD) solvers to get the same answers although the computation times are very much longer (Bencsik *et al* 2007, Gandhi

and Chen 1992, Li *et al* 2007). With the FDTD approach, in order to make computation times practical, a higher frequency of applied magnetic field is usually used. Whilst such a method will shorten computation times (as total time is related to frequency as well as length scales used), it is essential to ensure that the quasi-static conditions are still met and the appropriate (lower frequency) conductivity values are used by the software.

The authors cited in the above paragraph have used their various numerical methods to determine the electric fields induced in the human body during an MRI procedure. The choice of model and resolution can influence the peak currents flowing around the body (So *et al* 2004). This variation is noticeable specifically in the skin and fat layers where a 3 mm isotropic resolution may not be enough to adequately characterize the tissue. Unfortunately, these are the tissues where the sensory nerves may be being stimulated. However, the current densities and electric fields determined by these methods are in general of the order expected for stimulation given by the rheobase and chronaxie values determined experimentally. The regions stimulated are usually in general the regions with the highest electric field, e.g. the hips and lumbar region for y-axis gradient switching. What is still lacking is the full experimental verification of the numerical values of electric field at the sites of PNS for a given subject and their own individual body model. The conductivity models used in the above-cited numerical methods are based on a small set of available 'bodies' and resolutions.

Numerical simulations of trans-cranial magneto-stimulation (TMS) have been carried out by a number of authors (Wagner *et al* 2004). The numerical methods used for TMS are very similar as the quasi-static approximation is still valid although tissue permittivity is significant and can be modelled with a complex conductivity. The pulse times are usually shorter than the MRI switching times, which implies that TMS is working much higher up the response curve (figure 4) and hence peak induced currents are roughly an order of magnitude higher than for MRI PNS.

Measurement methods

The importance placed on analytic and numerical methods and their accurate prediction of current density in the human body is, in part, due to the difficulty of making accurate *in vivo* direct measurements. It is only feasible to conduct experiments either *in vitro*, in phantoms or in animals. Safety studies of electric fields have been carried out in this manner and current densities have been satisfactorily measured. However, the applied electric fields or directly applied potentials are both conservative in nature and reliable measurements can be made by simple probes (Miller 1991). These probes, assuming access is possible and little or no damage is caused to surrounding tissues, need to pay no regard to wire paths as there should be no induced EMF in the signal wires. Of course, every electro-physiologist knows the need to shield cables from extraneous electro-magnetic interference (EMI). When changing magnetic fields are introduced, the point measurement probes are no longer accurate. The induced electric field component tangential to the wire induces additional voltages in the wires. To determine the electric field correctly, a dipole probe has to be employed where the wires connecting the two tip points form a straight line (Hart and Wood 1991, Tofts and Branston 1991). The first *in vivo* measurements of electric fields induced by MRI scanner gradient switching have been described by Glover and Bowtell (2008). Figure 7 shows a segment from a pulse sequence where a calibrated pulse of 10 mT m^{-1} is used. The subject is positioned such that the magnetic field sensor (placed on the abdomen nearby) detects 1 T s^{-1} during the rise time of the pulse. The electric field generated on the surface of the abdomen is 0.15 V m^{-1}. An EPI sequence generates an electric field an order of magnitude greater at around 1.5 V m^{-1}. What is interesting is that the values measured are also in fairly close agreement with simple

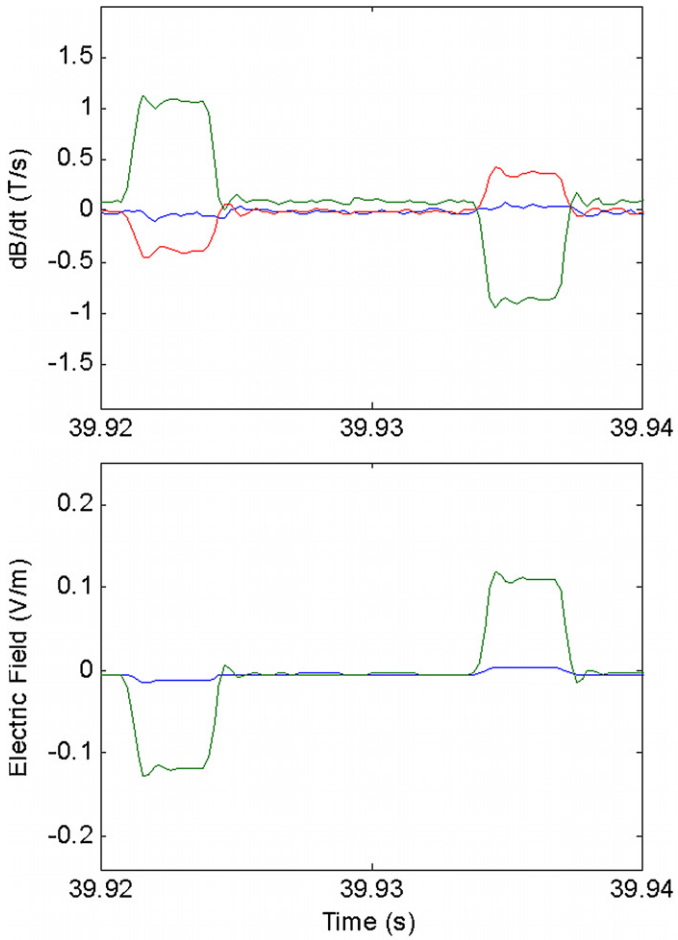

Figure 7. The magnetic field and induced electric field measured on a subject's abdomen whilst lying in a scanner. The graphs show a portion of gradient waveform where the rate of rise of gradient is 10 T m^{-1} s^{-1}. The axial and azimuthul electric field components are shown. Adapted from Glover and Bowtell (2008).

calculations based on the spherical model. The level of agreement depends on choosing a value of radius which corresponds to the size of the current loop around the body and gradient geometry. Glover and Bowtell (2008) also report results from an experiment where the subject is placed outside the scanner whilst the scanner is running an EPI sequence. As expected the coupling is a lot lower (and depends on exact positioning) yet values of measured electric field are comparable with numerical modelling as cited above. The measurements were for a single point and subject position and were generally smaller than the 1 cm^3 averaged values quoted from the numerical model papers (Li *et al* 2007, Riches *et al* 2007). In addition, the subject for the measurement was an unknown distance from the actual coil windings whereas the body model could be placed with greater accuracy and without regard for scanner fixtures.

It would be desirable to have a direct measurement of induced current using a similar probe. Current probes based on parallel plates are feasible but not practical *in vivo* (Deutsch

1968). As the current has to travel through the probe, the probe impedance has to mimic exactly that of the volume of tissue displaced. As this is not always known, it is possible that the probe itself will influence the current paths. In addition, the surface layer impedance of the probe is significant, meaning that the frequency response of the current probe is likely to be highly variable. In addition, very low frequency measurements are not practical. However, at gradient switching frequencies and for homogeneous phantoms, only this approach could be beneficial as a direct measurement method.

Regulatory issues

Guidelines for limits of exposure to electromagnetic radiation are set by (amongst others) the International Commission on Non-Ionising Radiation Protection (ICNIRP), the Institute of Electrical and Electronics Engineers (IEEE) and the International Electro-technical Commission (IEC). The Guidelines relevant to limits for frequencies covered by MRI gradient switching are ICNIRP (1998), IEEE International Committee on Electromagnetic Safety (ICES) (2002, 2005), and the IEC 60601-2-33 (2007). The European Union Physical Agents Directive (2004/40/EC) is largely based on the ICNIRP (1998) guidelines and concerns occupational exposures. This directive was due to be adopted from 1 May 2008 but has now been postponed until 2012 (2008/46/EC) after representation from the MRI community and others from within member states. The ICNIRP guidelines, and hence the EU directive, proposed a current density in tissue of 10 mA m^{-2} in the frequency range 10–1000 Hz and which scales with frequency up to 100 mA m^{-2} at 10 kHz (see table 1). The assumption made in the calculation is a tissue conductivity of 0.2 S m^{-1}. Hence, 10 mA m^{-2} would indicate an induced electric field of 50 mV m^{-1}. It is now feasible that the combination of *in vivo* surface electric field measurements and numerical modelling would indicate which procedures would exceed these values. As a response to concerns of the MR community, the EU commissioned a study of likely impacts due to implementation of the directive (Capstick *et al* 2008). The UK HSE also commissioned a study for numerical modelling from Stuart Crozier (Chadwick 2007). In both reports (and previous work cited above), it is clear from measurements and/or numerical modelling that for any person standing reasonably close to the end of the bore whilst the scanner is operating, the proposed limits would be exceeded (although exposure levels were generally below any PNS threshold). In clinical practice, it is not uncommon for a nurse, radiographer or accompanying person to be close to the bore during a scan in order to perform various tasks including administering contrast agents or keeping the patient calm. In interventional MRI, the surgeon or anaesthetist may be very close to the patient and within the volume of the scanner. Although the induced electric fields would exceed limits set by most regulatory bodies, these persons do not perceive PNS or magneto-phosphenes or are adversely affected in any way (disregarding the acoustic noise for which protection is available). As a separate issue, the movement of a person near the bore end of the magnet will also generate currents in excess of the currently proposed limit in EU Directive 2004/40/EC. The EU commissioned report (Capstick *et al* 2008) investigates such realistic scenarios. This report and the studies cited above indicate that gradient magnitudes would have to be reduced by factors between 2 and 10 for some procedures to be compliant with proposed occupational limits. The ICNIRP are currently reviewing their 'Guidelines on Limiting Exposure to Time-Varying Electric and Magnetic Fields (1 Hz to 100 kHz)' through a process of open consultation, and a report with revised guidelines is expected to be published in 2010 (www.icnirp.de).

The ICES guidelines are based on the induced electric field which does, at least, remove the unknown or assumed value of conductivity. Limits for electric field exposure (controlled

Table 1. Occupational exposure limit values for induced current density taken from EU directive 2004/40/EC.

Frequency, f (Hz)	RMS current density (mA m^{-2}) in central nervous tissues, averaged over 1 cm^2 normal to direction of current flow
0–1	40
1–4	$40/f$
4–1000	10
1 k–100 k	$f/100$

environment) are based on the known values for stimulation of electrically excitable tissue and (at 1 kHz) are 0.0177, 0.943 and 2.1 V m^{-1} RMS for brain, heart and other tissue respectively. These values of electric field would not cause PNS as they are safely below the rheobase value and are therefore deemed applicable for all frequencies or pulse lengths. However, the level set for brain CNS is based on the magneto-phosphene level at low frequency whereas experience indicates that no magnetophosphenes are perceived by subjects due to gradient switching. The IEC guidelines are simpler still with avoidance of PNS being the general issue. The scanner manufacturers generally follow the IEC guidelines for patient exposure (based on information available to the user). A threshold is determined by experiment to yield a value of the rate of change of magnetic field (or gradient) for which 50% of the population experience PNS. This threshold is then given a value of 100% beyond which the scanner will not allow. There are three modes which can be set: low (60%), moderate (80%) and high (100%) of that threshold value. In addition, there may be internal calculations which are used to predict the effect of a particular sequence based on a time constant nerve model (or similar) as discussed previously. These calculations may or may not use knowledge of the patient position in the scanner. It is unlikely that the geometry of the patient has been taken into account. Historically, in the absence of firm evidence for adverse effects other than PNS, manufacturers have taken no account of operator exposures—even for interventional systems—since if the scanner is set such that the patient does not experience PNS inside the scanner, then it is impossible that someone external to the bore could experience PNS even by extending their arm inside. The geometry of the arm (resulting in small current loops) and the gradient profile would ensure safe operation. An operator placing their head and/or trunk into the bore near a subject who is being scanned (but not experiencing PNS) could possibly exceed PNS threshold under certain conditions and such a practice should therefore be avoided. Open magnet systems give a greater opportunity for access to the gradient volume and hence possibility of an operator accessing regions of high switched magnetic gradient field. Usually such systems are not equipped with the highest performance gradient system, which does reduce the likelihood of the limits being exceeded.

Conclusions

The procedure of magnetic resonance imaging exposes the body to electromagnetic fields over a wide range of frequencies. Each frequency band affects a different biological response in the human body. In this review, the low (audio) frequencies associated with the imaging gradient switching and the main response of peripheral nerve stimulation has been examined in detail. Although the threshold limits (both magnitude and duration) for nerve stimulation are well known, there are still some difficulties in applying this knowledge to a specific system and

subject geometries—the latter being an ignored parameter. A better understanding of how to translate nerve level thresholds to scanner settings (from modelling and verification) is still needed in order to exploit the full capability of modern scanners without causing PNS to either subjects or operators. It should be feasible to take subject-specific geometry information and calculate electric fields for a given sequence and position inside a gradient coil in near real time. Threshold settings based on such a method would be tailored to the subject rather than a global population.

Acknowledgments

The author acknowledges the funding support of both the UK Medical Research and Engineering and Physical Sciences Research Councils.

References

Bailey W H and Nyenhuis J A 2005 Thresholds for 60 Hz magnetic field stimulation of peripheral nerves in human subjects *Bioelectromagnetics* **26** 462–8

Basser P J and Roth B J 2000 New currents in electrical stimulation of excitable tissues *Annu. Rev. Biomed. Eng.* **2** 377–97

Bencsik M, Bowtell R and Bowley R 2007 Electric fields induced in the human body by time-varying magnetic field gradients in MRI: numerical calculations and correlation analysis *Phys. Med. Biol.* **52** 2337–53

Bencsik M, Bowtell R and Bowley R M 2002 Electric fields induced in a spherical volume conductor by temporally varying magnetic field gradients *Phys. Med. Biol.* **47** 557–76

Bencsik M, Bowtell R and Bowley R M 2003 Using the vector potential in evaluating the likelihood of peripheral nerve stimulation due to switched magnetic field gradients *Magn. Reson. Med.* **50** 405–10

Bomhof C W and Van Der Vorst H A 2000 A parallel linear system solver for circuit simulation problems *Numer. Linear Algebr. Appl.* **7** 649–65

Bourland J D, Nyenhuis J A and Schaefer D L 1999 Physiologic effects of intense MR imaging gradient fields *Neuroimaging Clin. N. Am.* **9** 363–77

Bowtell R, Bencsik M and Bowley R 2003 Reducing peripheral nerve stimulation due to switched transverse field gradients using an additional concomitant field coil *Ann. Meeting of ISMRM (Toronto, Canada)* Abstract no 2424

Bowtell R and Bowley R M 2000 Analytic calculations of the E-fields induced by time-varying magnetic fields generated by cylindrical gradient coils *Magn. Reson. Med.* **44** 782–90

Budinger T F, Fischer H, Hentschel D, Reinfelder H E and Schmitt F 1991 Physiological-effects of fast oscillating magnetic-field gradients *J. Comput. Assist. Tomogr.* **15** 909–14

Capstick M *et al* 2008 An investigation into occupational exposure to electromagnetic fields for personnel working with and around medical magnetic resonance imaging equipment *Report* VT/2007/017 (Brussels: European Commission)

Cartee L A and Plonsey R 1992 The transient subthreshold response of spherical and cylindrical cell models to extracellular stimulation *IEEE Trans. Biomed. Eng.* **39** 76–85

Cavin I D, Glover P M, Bowtell R W and Gowland P A 2007 Thresholds for perceiving a metallic taste at large magnetic field *J. Magn. Reson. Imaging* **26** 1357–61

Chadwick P 2007 Assessment of electromagnetic fields around magnetic resonance imaging (MRI) equipment *Research Report* RR570 (London: Health and Safety Executive) http://www.hse.gov.uk/research/rrpdf/rr570.pdf

Cobos-Sanchez C 2007 Boundary element method for calculation of induced electric fields due to switched magnetic field gradients and movement in strong static fields *15th Ann. Meeting of the Int. Society for Magnetic Resonance in Medicine (Berlin)*

Cohen M S, Weisskoff R M, Rzedzian R R and Kantor H L 1990 Sensory stimulation by time-varying magnetic-fields *Magn. Reson. Med.* **14** 409–14

Collins C M, Li S Z and Smith M B 1998 SAR and B-1 field distributions in a heterogeneous human head model within a birdcage coil *Magn. Reson. Med.* **40** 847–56

Dawson T W, Caputa K and Stuchly M A 1997 Influence of human model resolution on computed currents induced in organs by 60-Hz magnetic fields *Bioelectromagnetics* **18** 478–90

Deford J F and Gandhi O P 1985 An impedance method to calculate currents induced in biological bodies exposed to quasi-static electromagnetic fields *IEEE Trans. Electromagn. Compat.* **27** 168–73

Den Boer J A, Bourland J D, Nyenhuis J A, Ham C L G, Engels J M L, Hebrank F X, Frese G and Schaefer D J 2002 Comparison of the threshold for peripheral nerve stimulation during gradient switching in whole body MR systems *J. Magn. Reson. Imaging* **15** 520–5

Deutsch S 1968 A probe to monitor electroanesthesia current density *IEEE Trans. Biomed. Eng.* **15** 130–1

Di Barba P, Mognaschi M E and Savini A 2007 Synthesizing a field source for magnetic stimulation of peripheral nerves *IEEE Trans. Magn.* **43** 4023–9

EU 2004 Physical Agents (Electromagnetic Fields) Directive 2004/40/EC (amended by 2008/46/EC) of the European Parliament and of the Council

Faber S C, Hoffmann A, Ruedig C and Reiser M 2003 MRI-induced stimulation of peripheral nerves: dependency of stimulation threshold on patient positioning *Magn. Reson. Imaging* **21** 715–24

Gandhi O P and Chen J Y 1992 Numerical dosimetry at power-line frequencies using anatomically based models *Bioelectromagnetics* **30** 43–60

Glover P M and Bowtell R 2007 Measurement of electric fields due to time-varying magnetic field gradients using dipole probes *Phys. Med. Biol.* **52** 5119–30

Glover P M and Bowtell R 2008 Measurement of electric fields induced in a human subject due to natural movements in static magnetic fields or exposure to alternating magnetic field gradients *Phys. Med. Biol.* **53** 361–73

Glover P M, Cavin I, Qian W, Bowtell R and Gowland P A 2007 Magnetic-field-induced vertigo: a theoretical and experimental investigation *Bioelectromagnetics* **28** 349–61

Ham C L G, Engels J M L, vandeWiel G T and Machielsen A 1997 Peripheral nerve stimulation during MRI: effects of high gradient amplitudes and switching rates *J. Magn. Reson. Imaging* **7** 933–7

Hart F X and Wood K W 1991 Eddy-current distributions—their calculation with a spreadsheet and their measurement with a dual dipole antenna probe *Am. J. Phys.* **59** 461–7

ICNIRP 1998 Guidelines for limiting exposure to time-varying electric, magnetic, and electromagnetic fields (up to 300 GHz) *Health Phys.* **74** 494–522

IEC 2007 *IEC std* 60601-2-33 am2 Ed. 2.0. (Geneva: IEC)

IEEE 2002 *IEEE Standard for Safety Levels with Respect to Human Exposure to Electromagnetic Fields, 0–3 kHz* C95.6-2002 (New York: Institute of Electrical and Electronics Engineers) p 43

Irnich W and Schmitt F 1995 Magnetostimulation in MRI *Magn. Reson. Med.* **33** 619–23

Jackson J D 1998 *Classical Electrodynamics* (New York: Wiley)

Lapicque L 1909 The experimental definition of stimulation *C. R. Seances Soc. Biol. Fil.* **67** 280–3

Li Y, Hand J W, Wills T and Hajnal J V 2007 Numerically-simulated induced electric field and current density within a human model located close to a z-gradient coil *J. Magn. Reson. Imaging* **26** 1286–95

Liu F and Crozier S 2004 A distributed equivalent magnetic current based FDTD method for the calculation of E-fields induced by gradient coils *J. Magn. Reson.* **169** 323–7

Liu F, Crozier S, Zhao H W and Lawrence B 2002 Finite-difference time-domain-based studies of MRI pulsed field gradient-induced eddy currents inside the human body *Concepts Magn. Reson.* **15** 26–36

Lovsund P, Oberg P A and Nilsson S E G 1980a Magnetophosphenes and electrophosphenes—a comparative study *Med. Biol. Eng. Comput.* **18** 758–64

Lovsund P, Oberg P A, Nilsson S E G and Reuter T 1980b Magnetophosphenes—a quantitative-analysis of thresholds *Med. Biol. Eng. Comput.* **18** 326–34

Maccabee P J, Amassian V E, Eberle L P and Cracco R Q 1993 Magnetic coil stimulation of straight and bent amphibian and mammalian peripheral-nerve *in vitro*—locus of excitation *J. Physiol.* **460** 201–19

Mansfield P and Harvey P R 1993 Limits to neural stimulation in echo-planar imaging *Magn. Reson. Med.* **29** 746–58

Mansfield P and Haywood B 2008 Controlled E-field gradient coils for MRI *Phys. Med. Biol.* **53** 1811–27

Mansfield P, Pykett I L, Morris P G and Coupland R E 1978 Human whole-body line-scan imaging by NMR *Br. J. Radiol.* **51** 921–2

Miller D L. 1991 Miniature-probe measurements of electric-fields and currents induced by a 60-Hz magnetic-field in rat and human models *Bioelectromagnetics* **12** 157–71

Mishra A, Joshi R P, Schoenbach K H and Clark C D 2006 A fast parallelized computational approach based on sparse LU factorization for predictions of spatial and time-dependent currents and voltages in full-body biomodels *IEEE Trans. Plasma Sci.* **34** 1431–40

Nadeem M, Thorlin T, Gandhi O P and Persson M 2003 Computation of electric and magnetic stimulation in human head using the 3D impedance method *IEEE Trans. Biomed. Eng.* **50** 900–7

Rattay F and Aberham M 1993 Modeling axon-membranes for functional electrical-stimulation *IEEE Trans. Biomed. Eng.* **40** 1201–9

Reilly J P 1989 Peripheral-nerve stimulation by induced electric currents—exposure to time-varying magnetic-fields *Med. Biol. Eng. Comput.* **27** 101–10

Riches S F, Collins D J, Scuffham J W and Leach M O 2007 EU directive 2004/40: field measurements of a 1.5 T clinical MR scanner *Br. J. Radiol.* **80** 483–7

Ruohonen J, Panizza M, Nilsson J, Ravazzani P, Grandori F and Tognola G 1996a Transverse-field activation mechanism in magnetic stimulation of peripheral nerves *Electroencephalogr. Clin. Neurophysiol. Electromyogr. Motor Control* **101** 167–74

Ruohonen J, Ravazzani P, Nilsson J, Panizza M, Grandori F and Tognola G 1996b A volume-conduction analysis of magnetic stimulation of peripheral nerves *IEEE Trans. Biomed. Eng.* **43** 669–78

Schaefer D J, Bourland J D and Nyenhuis J A 2000 Review of patient safety in time-varying gradient fields *J. Magn. Reson. Imaging* **12** 20–9

Schenck J F, Edelstein W A, Hart H R, Williams C S, Bean C P, Bottomley P A and Redington R W 1983 Switched gradients and rapidly changing magnetic-field hazards in NMR imaging *Med. Phys.* **10** 133–133

So P P M, Stuchly M A and Nyenhuis J A 2004 Peripheral nerve stimulation by gradient switching fields in magnetic resonance imaging *IEEE Trans. Biomed. Eng.* **51** 1907–14

Tofts P S and Branston N M 1991 The measurement of electric-field, and the influence of surface-charge, in magnetic stimulation *Electroencephalogr. Clin. Neurophysiol.* **81** 238–9

Ueno S, Harada K, Ji C and Oomura Y 1984 Magnetic nerve-stimulation without interlinkage between nerve and magnetic-flux *IEEE Trans. Magn.* **20** 1660–2

Wagner T A, Zahn M, Grodzinsky A J and Pascual-Leone A 2004 Three-dimensional head model simulation of transcranial magnetic stimulation *IEEE Trans. Biomed. Eng.* **51** 1586–94

Wang H, Liu F, Xia L and Crozier S 2008 An efficient impedance method for induced field evaluation based on a stabilized Bi-conjugate gradient algorithm *Phys. Med. Biol.* **53** 6363–75

Weiss G 1901 The law of electrical stimulation in the nerves *C. R. Seances Soc. Biol. Fil.* **53** 466–8

Zhang B B, Yen Y F, Chronik B A, McKinnon G C, Schaefer D J and Rutt B K 2003 Peripheral nerve stimulation properties of head and body gradient coils of various sizes *Magn. Reson. Med.* **50** 50–8